ACS central science

Research Article

Cite This: ACS Cent. Sci. 2019, 5, 1541−1553

http://pubs.acs.org/journal/acscii

Construction of a Fluorescent Screening System of Allosteric Modulators for the $GABA_A$ Receptor Using a Turn-On Probe

Seiji Sakamoto,[†] Kei Yamaura,[†,⊥] Tomohiro Numata,[‡] Fumio Harada,[†] Kazuma Amaike,[†] Ryuji Inoue,[‡] Shigeki Kiyonaka,[†,#] and Itaru Hamachi*[,†,§]

[†]Department of Synthetic Chemistry and Biological Chemistry, Graduate School of Engineering, Kyoto University, Katsura, Nishikyo-ku, Kyoto 615-8510, Japan

[‡]Department of Physiology, School of Medicine, Fukuoka University, 7-45-1 Nanakuma, Jonan-ku, Fukuoka 814-0180, Japan

[§]ERATO Innovative Molecular Technology for Neuroscience Project, Japan Science and Technology Agency (JST), Kyoto 615-8530, Japan

Supporting Information

ABSTRACT: γ-Aminobutyric acid (GABA) is the major inhibitory neurotransmitter in the central nervous system. The fast inhibitory actions of GABA are mainly mediated by $GABA_A$ receptors ($GABA_A$Rs), which are widely recognized as clinically relevant drug targets. However, it remains difficult to create screening systems for drug candidates that act on $GABA_A$Rs because of the existence of multiple ligand-binding sites and the delicate pentameric structures of $GABA_A$Rs. We here developed the first turn-on fluorescent imaging probe for $GABA_A$Rs, which can be used to quantitatively evaluate ligand−receptor interactions under live cell conditions. Using noncovalent labeling of $GABA_A$Rs with this turn-on probe, a new imaging-based ligand assay system, which allows discovery of positive allosteric modulators (PAMs) for the $GABA_A$R, was successfully constructed. Our system is applicable to high-throughput ligand screening, and we discovered new small molecules that function as PAMs for $GABA_A$Rs. These results highlight the power of the use of a turn-on fluorescent probe to screen drugs for complicated membrane proteins that cannot be addressed by conventional methods.

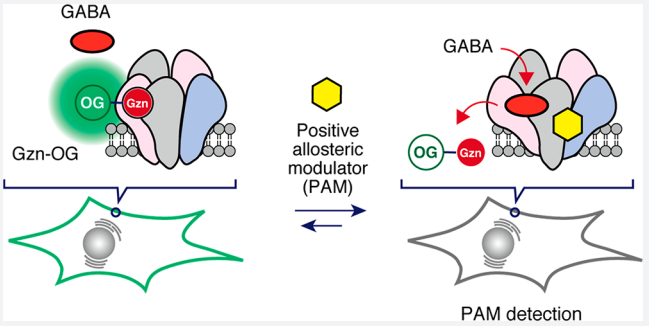

INTRODUCTION

Allosteric modulators have recently drawn intense attention in new drug development.[1,2] These molecules bind to sites distinct from the highly conserved endogenous ligand-binding (orthosteric) site of a target protein or enzyme, to regulate positively or negatively the affinity of the orthosteric ligand. Allosteric modulators are expected to show lower toxicity and higher specificity compared with competitive orthosteric ligands, because allosteric ligands can function in the limited spatiotemporal conditions in which the orthosteric ligand is present in vivo. However, methods for discovering allosteric modulators for a specific target protein are still very limited.[1,3] Evaluation of the allosteric binding of chemical compounds is conducted by X-ray crystallography,[4] H/D exchange mass spectrometry,[5] and NMR,[6] which are difficult methods to apply to membrane proteins because of their structural complexity and large molecular size. The affinity-ratio assay allows for the detection of the allosteric effects of modulators for membrane proteins.[7,8] This assay requires a membrane fraction expressing a target receptor, an allosteric modulator (candidate), an orthosteric agonist, and a radioactive antagonist that is bound to the orthosteric site. The binding of the radioactive antagonist to the membrane fraction containing the target protein is impacted by the orthosteric agonist, whose affinity is altered with allosteric modulators. Potent allosteric modulators can be identified by the differences in the bound radioactive antagonist, in the presence or absence of the allosteric modulator, at a fixed concentration of the orthosteric agonist. Although useful, this radioisotope assay is not suitable for the rapid and high-throughput screening of a library of small molecules. Moreover, the filtration and washing-out processes hamper the use of radioactive ligands with low affinity (K_d > μM).[9] As many orthosteric ligands for neurotransmitter receptors exhibit rather low affinity (K_d values in the order of tens of μM), application of the affinity-ratio assay is seriously limited for such proteins.

Allosteric modulators that act on the central nervous system have been widely used as anxiolytic and sleeping agents, and as therapeutic agents for Alzheimer's disease because they do not disturb neural transmission.[10,11] One of the main targets of these modulators is a $GABA_A$ receptor ($GABA_A$R) acting as a major inhibitory neurotransmitter receptor (Figure 1a).[12,13]

Received: June 1, 2019
Published: August 16, 2019

DOI: 10.1021/acscentsci.9b00539
ACS Cent. Sci. 2019, 5, 1541−1553

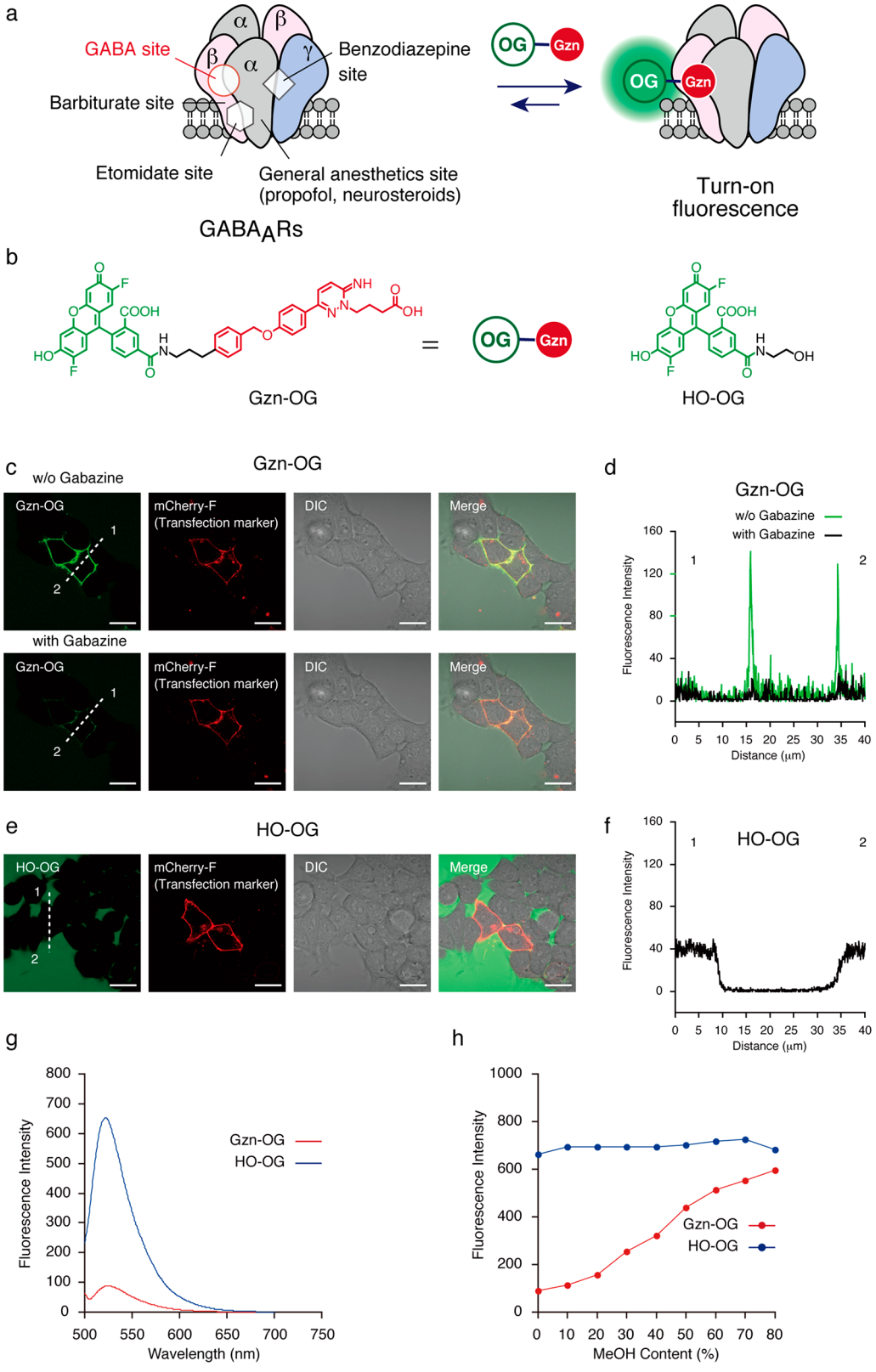

Figure 1. Characterization of a turn-on fluorescent imaging probe Gzn-OG. (a) Schematic illustration of a turn-on fluorescent probe for GABA$_A$Rs. (b) Chemical structure of a turn-on fluorescent imaging probe, Gzn-OG, and a control fluorophore, HO-OG. (c and e) Confocal live cell imaging of HEK293T cells transfected with GABA$_A$R(α1/β3/γ2) upon addition of Gzn-OG (1 μM) (c) and HO-OG (1 μM) (e) in the presence or absence of gabazine (100 μM). Scale bar = 40 μm. (d and f) Fluorescence intensity analyses of the confocal images for Gzn-OG (d) and HO-OG (f). (g) Fluorescence spectra of Gzn-OG (1 μM) or HO-OG (1 μM) in HBS buffer (pH 7.4) at r.t. λ_{ex} = 496 nm. (h) Plots of fluorescence intensities at peak tops with increasing MeOH content. See Figure S3b,c for these fluorescence spectra.

DOI: 10.1021/acscentsci.9b00539
ACS Cent. Sci. 2019, 5, 1541−1553

Benzodiazepines are positive allosteric modulators (PAMs) of $GABA_AR$s and are widely used in the treatment of epilepsy, insomnia, anxiety, and panic disorder.[14,15] Barbiturates, volatile and intravenous anesthetics, neurosteroids, and ethanol are all allosteric modulators that can modulate the affinity of GABA (an orthosteric ligand) to $GABA_AR$s.[16] However, these drugs often cause problematic drug resistance and addiction in vulnerable individuals.[17−21] In addition, overdose mortality involving benzodiazepines has increased considerably in recent years.[22] Recently, we reported a method for screening small molecules capable of binding to $GABA_AR$, using fluorescent turn-on $GABA_AR$-based sensors under live cell conditions.[23] These biosensors were constructed by a combination of the chemical labeling of $GABA_AR$s by ligand-directed acyl imidazole (LDAI) chemistry[24] and a bimolecular fluorescence quenching and recovery (BFQR) method (Figure S1a).[25] Although useful, this system gave relatively small fluorescence changes upon ligand binding and required tedious protein-labeling protocols and time-consuming processes for Förster resonance energy transfer (FRET) system construction. More simple and rapid methods for assaying ligand−$GABA_AR$ interactions are highly desirable.

Here, we describe the development of the first turn-on fluorescence imaging probe for the $GABA_AR$ that consists of an Oregon Green (OG) fluorophore and a gabazine antagonist (Figure 1b). A new ligand assay system was successfully constructed on the basis of the noncovalent labeling of $GABA_AR$ with this fluorescent probe in live cells. This biosensor allows the detection of positive allosteric modulators (PAMs) for the $GABA_AR$ using the changes in the affinity of an orthosteric ligand that can be induced by allosteric modulators. Because of its simplicity, our fluorescence assay system was readily applicable to the high-throughput screening of a library of pharmacologically active compounds in live cells, which enabled the discovery of new small molecules that can act as PAMs for $GABA_AR$s.

RESULTS

Turn-On Fluorescence Properties of the Imaging Probe, Gzn-OG. During the chemical labeling of $GABA_AR$s on live HEK293T cells, we noticed the LDAI reagent CGAM-Gzn (targeting a GABA binding site, as shown in Figure S1b)[23] exhibited a turn-on fluorescence property, using confocal laser scanning microscopy (CLSM). Pronounced fluorescence was observed from the plasma membrane of HEK293T cells transfected with the $\alpha1$, $\beta3$, and $\gamma2$ subunits of $GABA_AR$s ($GABA_AR(\alpha1/\beta3/\gamma2)$) upon addition of CGAM-Gzn without a washing operation, whereas rather low fluorescence was detected from the extracellular space (Figure S1c (left image)). Such turn-on fluorescence was not observed by addition of the same concentration of other labeling reagents, such as CGAM-Bzp, which targets the benzodiazepine binding site, where strong fluorescence was exhibited from the extracellular regions as well as from the membrane region (Figure S1d (left image)). To evaluate the turn-on fluorescence property of CGAM-Gzn in detail, we prepared the imaging probe, Gzn-OG, in which a gabazine derivative was simply linked to an OG fluorophore without the reactive acyl imidazole moiety (Figure 1b). Similar to CGAM-Gzn, strong fluorescence was observed only from the cell surface, without washing, when Gzn-OG was applied to $GABA_AR(\alpha1/\beta3/\gamma2)$ in live HEK293T cells (Figure 1c). The fluorescence intensity on the cell surface remarkably decreased upon addition of gabazine, while the fluorescence intensity was negligibly changed in the extracellular region (Figure 1c). These imaging data for Gzn-OG clearly indicated that the turn-on fluorescence occurred via binding to $GABA_AR$s on live HEK293T cells, and the on/off switching was reversible. In addition, Gzn-OG is not cell permeable, allowing $GABA_AR$s to be visualized on the cell surface without any washing operations. In contrast, high background signals were observed from the extracellular regions when the probe lacking the gabazine group (HO-OG) and the probe possessing a benzodiazepine derivative (Bzp-OG) were used (Figures 1e and S2). The line plot analysis of the CLSM images revealed that the background intensity of Gzn-OG was about four times smaller than those of HO-OG and Bzp-OG under the same conditions (Figures 1d,f and S2c).

The photochemical properties of the imaging probes were examined by UV−vis absorption and fluorescence spectroscopy in aqueous buffer solution (Figures 1g,h, S2d, and S3). Gzn-OG, Bzp-OG, and HO-OG exhibited almost the same UV−vis spectra in the 300−550 nm range (Figure S3a, left), whereas the fluorescence intensity of Gzn-OG was significantly less than those of Bzp-OG and HO-OG (Figures 1g and S2d). When an aqueous solution of Gzn-OG was mixed with methanol, an increase in the methanol content from 0% to 80% resulted in an approximately 6-fold increase in the fluorescent intensity of Gzn-OG without substantial changes in the UV−vis spectral properties (Figures 1h and S3b). In contrast, there were negligible changes in the fluorescence spectra of HO-OG and Bzp-OG on mixing with methanol (Figures 1h, S2e, and S3c,d). These results suggested the fluorescence of Gzn-OG was quenched in the aqueous solution possibly because of the intramolecular stacking between the OG and gabazine moieties. The binding of the gabazine moiety to $GABA_AR$s could facilitate the conformational change of the Gzn-OG probe leading to the fluorescence recovery in the extended form. Intermolecular aggregation of Gzn-OG was unlikely because a linear relationship between the fluorescence intensity (or absorbance), and the probe concentration in the range of 0.1−10 μM was observed for Gzn-OG (Figure S4). As shown in Figure S5, the Gzn-OG exhibited a weaker fluorescence than the labeling reagent CGAM-Gzn in the buffer, suggesting the shorter linker is preferable for the more efficient fluorescence quenching. We also varied the fluorophore part of the Gzn-probe, such as Gzn-Fl, Gzn-Ax488, Gzn-Ax647, and Gzn-DBD that bear 5-carboxyfluorescein (Fl), Alexa Fluor 488 (Ax488), Alexa Fluor 647 (Ax647), and 4-(*N*,*N*-dimethylaminosulfonyl)-7-aminobenzoxadiazole (DBD), respectively (Figures S6, S7, S8, and S9). Like Gzn-OG, the spectroscopic measurement of Gzn-Fl and Gzn-Ax488 suggested their turn-on property, and the CLSM study by them indeed allowed for the turn-on fluorescence imaging of $GABA_AR(\alpha1/\beta3/\gamma2)$ on live cells (Figures S6 and S7). It was also noted that Gzn-OG exhibited the lowest background signals among them. In contrast, Gzn-Ax647 and HO-Ax647 showed almost identical fluorescence intensities in the buffer, suggesting that Gzn-Ax647 did not have a turn-on fluorescent property (Figure S8g). However, CLSM imaging showed the strong fluorescence on live cells expressing $GABA_AR$s, while the background signal was relatively low. It may be due to a distinct mechanism for turn-on fluorescence upon $GABA_AR$ binding. In the case of an environment-sensitive DBD (Gzn-DBD) which was utilized for proteins detection in test tubes,[26] it did not work as the turn-on $GABA_AR$ imaging probe under the live cells conditions,

DOI: 10.1021/acscentsci.9b00539
ACS Cent. Sci. 2019, 5, 1541−1553

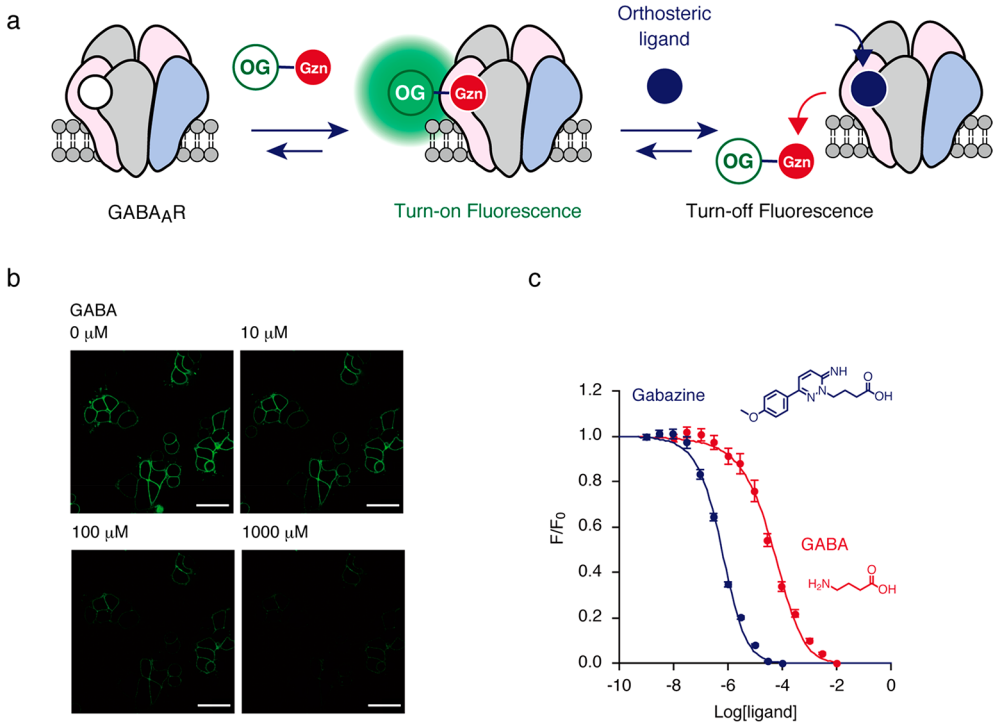

Figure 2. Competitive binding assay of orthosteric ligands using Gzn-OG. (a) Schematic illustration of competitive binding assay using Gzn-OG. (b) Confocal live cell imaging of HEK293T cells transfected with GABA$_A$R(α1/β3/γ2) upon addition of Gzn-OG (100 nM) at various concentrations of GABA. Scale bar = 40 μm. (c) Plots of fluorescence intensity (F/F_0) of plasma membranes of cells with increasing ligand concentration. HEK293T cells transfected with GABA$_A$R(α1/β3/γ2) were treated with 100 nM Gzn-OG, and then the fluorescence intensity of cells was measured by confocal microscopy with increasing GABA or gabazine concentration. The K_d values of GABA and gabazine for GABA$_A$R(α1/β3/γ2) were determined to be 16.9 μM and 214 nM, respectively, by fitting the fluorescence change with a logistic equation. For details, see Methods. n = 12. Data represent mean ± SEM.

while it showed strong solvent-dependent changes of the fluorescence in test tube experiments (Figure S9).

The binding affinity of Gzn-OG to the GABA$_A$R(α1/β3/γ2) in live HEK293T cells was determined by CLSM imaging. Two-fold serial dilutions of Gzn-OG in the cell culture dish resulted in a gradual decrease in the fluorescence intensity from the cell membrane because of the reversible binding of Gzn-OG to GABA$_A$R(α1/β3/γ2) (Figure S10). Fitting the fluorescence intensity change with the decrease in the Gzn-OG concentration gave a dissociation constant (K_d) of 54.9 nM, which was comparable to previously reported values for gabazine derivatives (2−280 nM).[27,28] This result indicated that the chemical conjugation of the OG fluorophore to Gzn does not appreciably affect the affinity of the gabazine ligand for GABA$_A$Rs.

We further examined the subunit specificity of Gzn-OG using HEK293T cells transfected with varied compositions of the subunits (a single subunit, α1, β3, or γ2; two subunits of α1 and β3 (α1/β3), α1 and γ2 (α1/γ2), or β3 and γ2 (β3/γ2)). Among them, the pentamers of β, α/β, α/γ, β/γ, and $\alpha/\beta/\gamma$ have been previously revealed to retain both their ion-channel activity and ligand-binding capability.[29,30] The prominent fluorescence was only observed from the cell surfaces expressing α1/β3 or β3/γ2, in addition to α1/β3/γ2 (Figure S11). These results were consistent with those previously observed in the Western blotting analysis of the chemically labeled GABA$_A$R(β3/γ2) using the CGAM-Gzn reagent.

On-cell Binding Assay of Orthosteric Ligands Using Gzn-OG. With a reversible turn-on fluorescent probe in hand, an imaging-based ligand-binding assay was performed (Figure 2a). After the staining of GABA$_A$Rs with Gzn-OG (100 nM) under live cell conditions, orthosteric ligands, such as GABA (agonist) and gabazine (antagonist), were added to the culture medium, and changes in the fluorescence images were monitored by CLSM without washing operations. When GABA was added to the culture medium, a significant decrease in fluorescence intensity at the cell surface was induced in a concentration-dependent manner, suggesting that GABA excluded Gzn-OG from the orthosteric binding site in a competitive manner (Figure 2b). In the case of gabazine, a strong antagonist, a similar fluorescence decrease was observed in the CLSM image, which reached saturation at approximately 10 μM (Figure S12). From the fluorescence titration curves of these assays in live cells, the K_d values of GABA and gabazine were determined to be 16.9 μM and 214 nM, respectively (Figure 2c). These values were almost identical to those previously determined by function-based assays using live cells (K_d = 26−42 μM[31,32] and 210−280 nM[27,28] for GABA and gabazine, respectively), demonstrating that the fluorescence turn-on probe, Gzn-OG, is valuable not only for the imaging of membrane-bound GABA$_A$Rs but also for quantitative analysis of orthosteric ligands for GABA$_A$Rs under live cells conditions.

On-cell Binding Assay of PAMs for the GABA$_A$R using Gzn-OG. Next, we sought to create a ligand assay system for PAMs of GABA$_A$Rs using Gzn-OG (Figure 3a). We here exploited a unique character of PAMs that can enhance the affinity of orthosteric agonists but not antagonists to the receptors.[33] On the basis of the titration data from a competitive assay for GABA, 100 nM Gzn-OG was

DOI: 10.1021/acscentsci.9b00539
ACS Cent. Sci. 2019, 5, 1541−1553

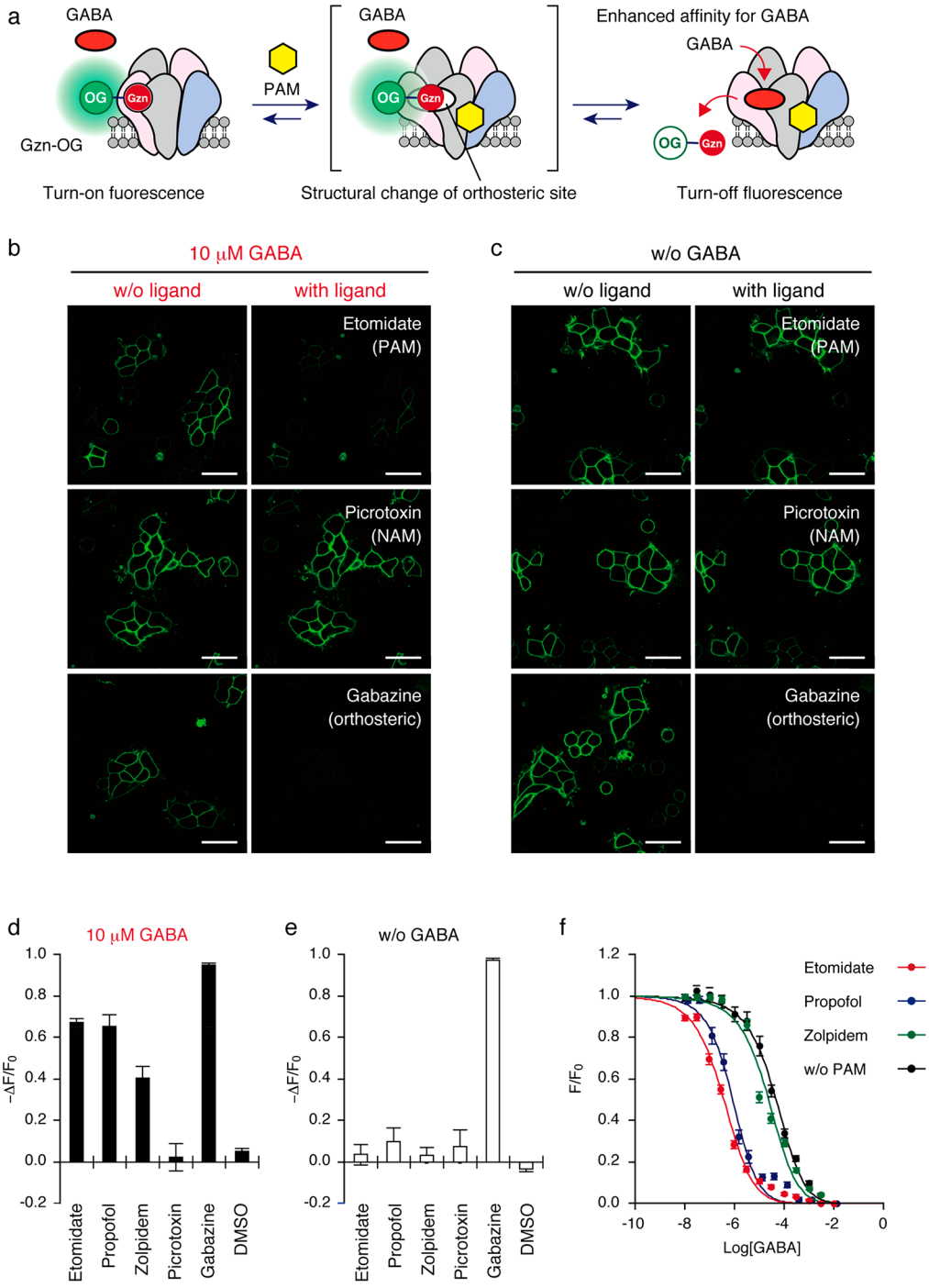

Figure 3. Detection of PAMs for $GABA_AR(\alpha1/\beta3/\gamma2)$ using Gzn-OG. (a) Schematic illustration of the assay system for detecting PAMs. (b, c) Ligand induced CLSM imaging change in the presence (b) or absence (c) of GABA. The cells were treated with 100 nM Gzn-OG, and then ligand (200 μM etomidate (PAM), 20 μM picrotoxin (NAM) or 100 μM gabazine (orthosteric antagonist)) was added in the presence (b) or absence (c) of 10 μM GABA. Scale bar = 40 μm. (d and e) Fluorescence changes after adding various types of $GABA_AR$ ligands in the presence (d) or absence (e) of GABA (10 μM). The fluorescent intensity change ($-\Delta F/F_0$) after addition of each ligand is shown. Each ligand concentration is as follows: etomidate (200 μM), propofol (200 μM), zolpidem (20 μM), picrotoxin (20 μM), and gabazine (100 μM). Data represent mean ± SEM n = 10–12. (f) Plots of fluorescence intensity (F/F_0) of plasma membranes of cells with increasing GABA concentration. HEK293T cells transfected with $GABA_AR(\alpha1/\beta3/\gamma2)$ were treated with 100 nM Gzn-OG and each PAM, and then the fluorescence intensity of cells was measured by confocal microscopy with increasing GABA concentration. The EC_{50} and K_d values of GABA in the presence of each PAM were determined by fitting the fluorescence change with a logistic equation. For details, see Methods. n = 12. Data represent mean ± SEM K_d values for GABA were determined to be 0.13, 0.23, 8.1, and 16.9 μM in the presence of PAM (etomidate, propofol, or zolpidem), or absence of PAM, respectively.

coincubated together with 10 μM GABA in HEK293T cells expressing $GABA_AR(\alpha1/\beta3/\gamma2)$; at this concentration, most of the Gzn-OG remained in the orthosteric binding site of the $GABA_AR$ (Figure S13). The affinity of GABA to $GABA_AR$ is allosterically enhanced upon addition of a PAM, so that the competitive replacement of Gzn-OG with GABA would be

DOI: 10.1021/acscentsci.9b00539
ACS Cent. Sci. 2019, 5, 1541−1553

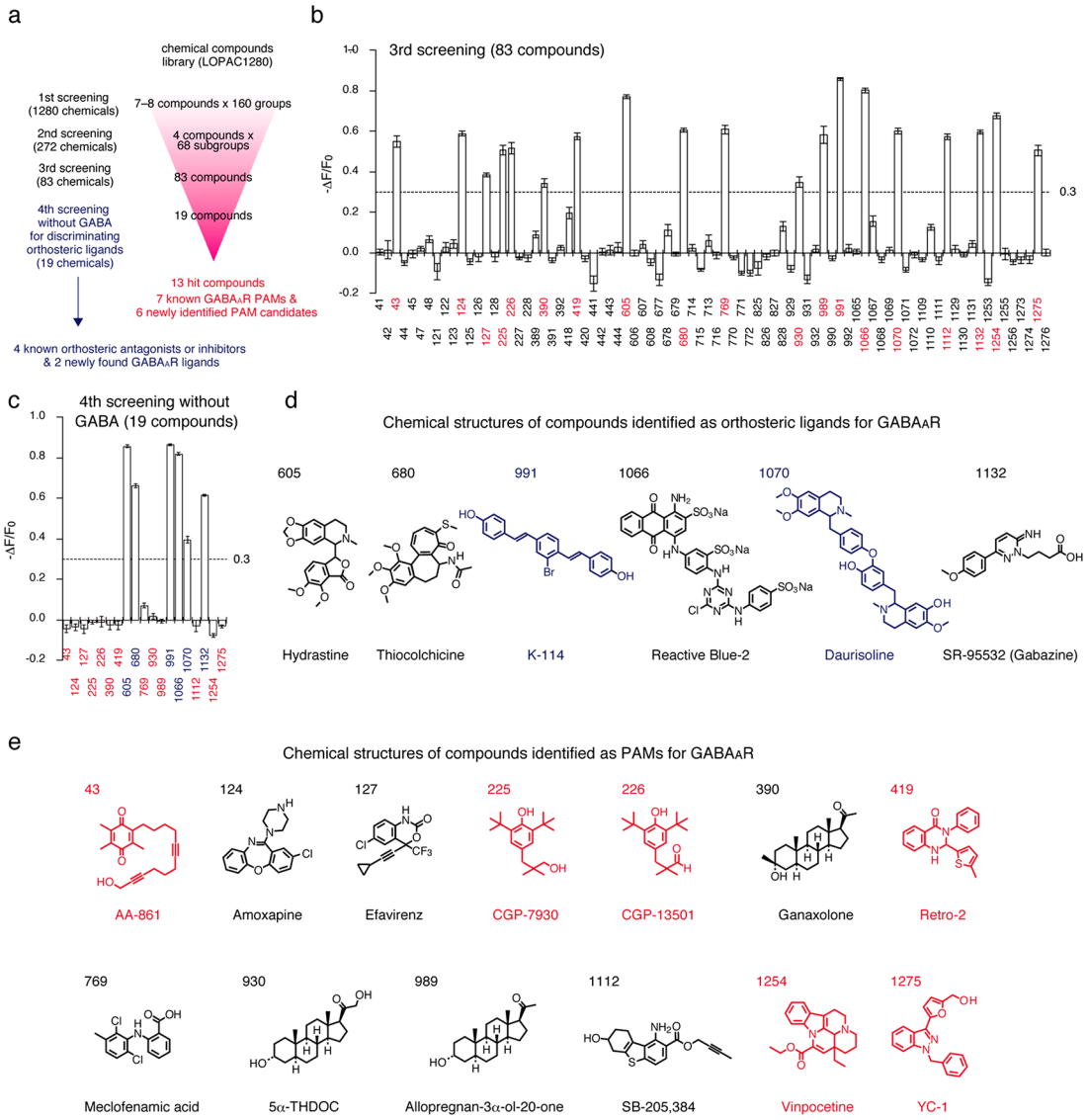

Figure 4. High-throughput screening of PAMs for GABA$_A$R($\alpha1/\beta3/\gamma2$) by a ligand assay system using Gzn-OG. (a) Flowchart of the screening process from a chemical library containing 1280 compounds. Chemical information on the library is listed in Table S1. (b) $-\Delta F/F_0$ values in the third screening process. In this process, the ligand assay system was treated with 10 μM of each compound in the presence of 10 μM GABA. Threshold ($-\Delta F/F_0 = 0.3$) in this screening is shown as a dashed line. Data represent mean ± SEM n = 8−12. Hit compounds are marked in red. (c) $-\Delta F/F_0$ values in the fourth screening process. In this process, the ligand assay was performed in the absence of GABA by treating with 10 μM of each hit compound found in the third screening process. Threshold ($-\Delta F/F_0 = 0.3$) in this screening is shown as a dashed line. Data represent mean ± SEM n = 8−12. Hit compounds identified as orthosteric ligands and PAMs are marked in blue and red, respectively. (d) Chemical structures of hit compounds identified as orthosteric ligands for GABA$_A$Rs in the screening assay. Newly identified GABA$_A$R ligands via this screening assay are shown in blue. (e) Chemical structures of hit compounds identified as PAMs for GABA$_A$Rs in the screening assay. Newly identified PAM candidates via this screening assay are shown in red.

facilitated, causing a decrease in the fluorescence intensity in the cell-membrane region (Figure 3a). As a proof-of-principle, the fluorescence change ratio ($\Delta F/F_0$) was evaluated upon addition of well-known PAMs for the GABA$_A$R, such as zolpidem (20 μM), etomidate (200 μM), and propofol (200 μM) (Figure S14a). Addition of these PAMs to the culture medium resulted in a negligible fluorescence change in the absence of GABA (Figure 3c,e), whereas a pronounced fluorescent decrease was observed in the presence of 10 μM GABA (Figure 3b,d). In contrast, picrotoxin, a representative negative allosteric modulator (NAM),[33] had no effect on the fluorescence intensity, both in the presence and absence of 10 μM GABA. Gabazine (an orthosteric antagonist) induced a significant decrease in the $\Delta F/F_0$ value, both in the presence and absence of 10 μM GABA, indicating that such a competitive ligand was easily discriminated from PAMs (Figure 3b−e). These results clearly implied that the fluorescence turn-on probe Gzn-OG, with a reversible binding property, is a powerful agent for determining PAMs for GABA$_A$Rs.

This assay system allowed for the quantitative analysis of the pharmacological properties of PAMs. The fluorescent changes resulting from Gzn-OG with varying concentrations of GABA were monitored in the presence of PAMs to evaluate their effect on the GABA affinity to GABA$_A$R($\alpha1/\beta3/\gamma2$) (Figure S14b). The concentration−response curves were shifted to the left upon addition of PAMs in all cases, confirming that these compounds were indeed PAMs (Figure 3f). The K_d values for

DOI: 10.1021/acscentsci.9b00539
ACS Cent. Sci. 2019, 5, 1541−1553

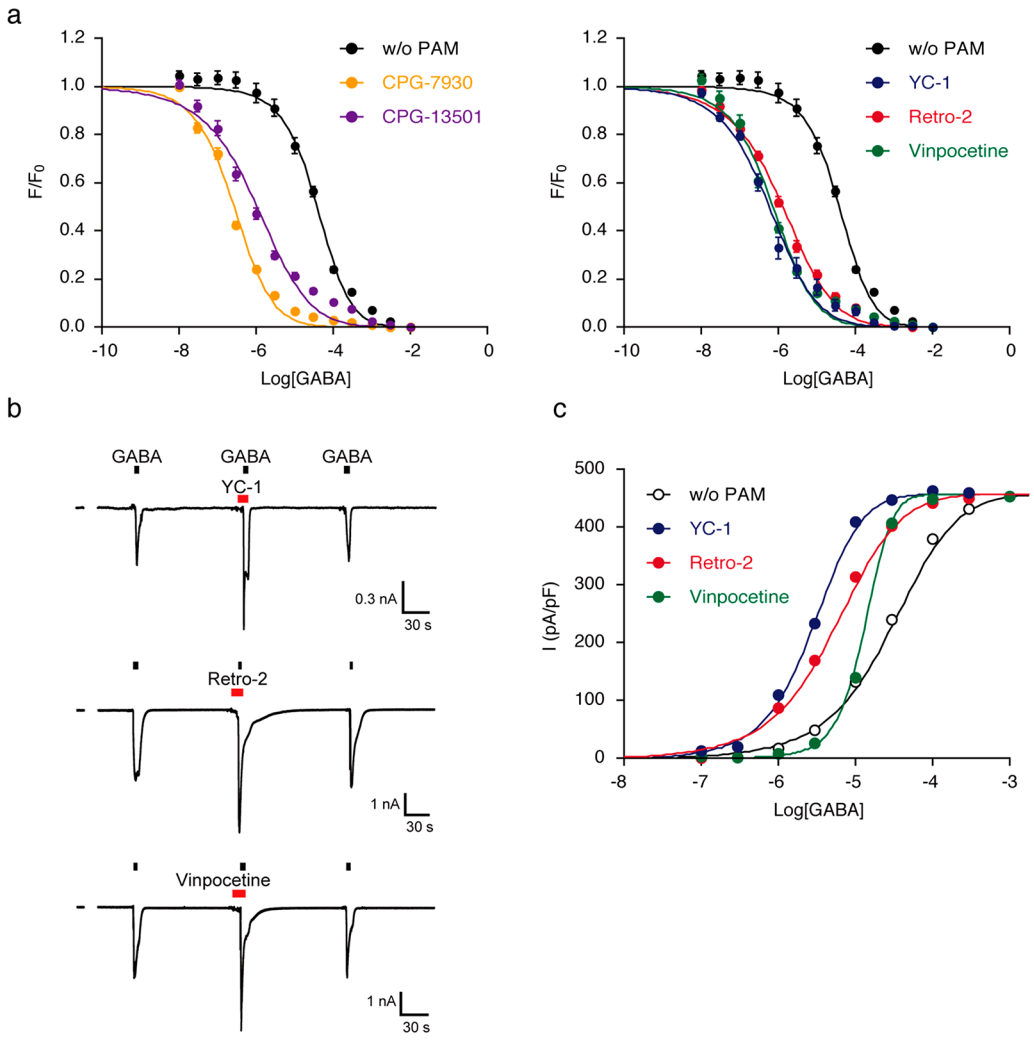

Figure 5. Functional characterization of hit compounds. (a) Plots of fluorescence intensity (F/F_0) of plasma membranes of cells with increasing GABA concentration in the presence or absence of each hit compound (25 μM). HEK293T cells transfected with $GABA_AR(\alpha1/\beta3/\gamma2)$ were treated with 100 nM Gzn-OG and 25 μM hit compound, and then the fluorescence intensity of cells was measured by confocal microscopy with increasing GABA concentration. The K_d value of GABA in the presence of each hit compound was determined by fitting the fluorescence change with a logistic equation. n = 10. Data represent mean ± SEM K_d values for GABA were determined to be 0.095, 0.38, 0.26, 0.46, and 0.21 μM for CGP-7930, CGP-13501, vinpocetine, Retro-2 and YC-1, respectively. (b) Effects of compounds on the whole-cell currents in $GABA_AR(\alpha1/\beta3/\gamma2)$-transfected HEK293T cells. Representative time courses of the GABA-induced currents at −60 mV by the addition of YC-1, Retro-2 or vinpocetine are shown. [compound] = 3 μM and [GABA] = 30 μM. (c) Dose−response curves for peak GABA-induced current in the absence or presence of 3 μM vinpocetine, YC-1 or Retro-2. EC_{50} values were determined to be 13.7, 2.8, 4.8, and 27.8 μM in the presence of PAM (vinpocetine, YC-1 or Retro-2), or absence of PAM, respectively.

GABA determined from these curves were 0.13, 0.23, and 8.1 μM in the presence of etomidate, propofol, and zolpidem, respectively. These shifted K_d values for GABA were almost same as data previously determined by function-based assays in live cells (K_d = 0.79, 0.5, and 13 μM with etomidate,[34] propofol,[35] and zorpidem,[36] respectively). In addition, the concentration-dependency of these PAMs assessed by our assay system (Figure S14c) gave K_d values for etomidate and propofol of 2.7 and 5.6 μM, respectively. These values were again almost comparable to the K_d values previously reported using live cells (K_d = 1.8 and 1.9 μM, respectively).[37,38] Overall, these results indicated that our $GABA_AR$ ligand assay system relying on a turn-on fluorescent probe enabled the selective and quantitative characterization of PAMs in live cells.

Screening of Small Molecules as $GABA_AR$ Ligands. Using this simple and convenient ligand assay system, we attempted to discover new ligands that can function as PAMs for $GABA_ARs$ from a library of pharmacologically active compounds (LOPAC1280). Gzn-OG (100 nM) and GABA (10 μM) were coincubated in HEK293T cells transfected with $GABA_AR(\alpha1/\beta3/\gamma2)$, and the fluorescence changes upon addition of the small molecules were monitored by CLSM under live cell conditions. The assay was performed in three different steps to enhance the screening efficiency (Figure 4a). We conducted an additional fluorescent assay (fourth screening) in the absence of GABA to discriminate compounds competitively bound to the orthosteric (GABA) binding site. In the first screening, seven or eight different compounds were mixed in the same tube, and 160 groups of the resulting mixture were added to the cell-based assay system. A pronounced decrease in the fluorescence intensity of the cell membrane was detected in 34 groups, which showed a defined threshold ($-\Delta F/F_0 > 0.5$) (Figure S15a). In the second step, each hit group was divided into two subgroups to confer a total

DOI: 10.1021/acscentsci.9b00539
ACS Cent. Sci. 2019, 5, 1541−1553

of 68 subgroups containing four compounds. Monitoring the fluorescence change induced by each subgroup ($-\Delta F/F_0$ > 0.4) resulted in identification of 21 hit groups (Figure S15b). In the third screening step, each compound (83 in total) was separately added to our assay system; 19 compounds exhibited a pronounced fluorescence decrease ($-\Delta F/F_0$ > 0.3) (Figure 4b). Finally, these compounds were subjected to the fourth screening step in the absence of GABA to detect orthosteric ligands (Figure 4c), which left 13 compounds identified as PAMs for $GABA_AR$s (Figure 4e). We determined the threshold values to leave ∼20% of groups or compounds as hits for performing the screening efficiently. Based on the statistical Z-factor analysis,[39] the averaged *Z*-factor values were determined to be 0.850, 0.834, 0.799, and 0.891 for the first, second, third, and negative selections, respectively (Supporting Table S2), and each hit group or compound in all screening steps showed the *Z*-factor value to be within the range of 0.60 < *Z* < 0.93. These indicated all screening steps were carried out with strict and robust criteria.

On the basis of the supplied LOPAC1280 list, 7 of the 13 PAM candidates were already known PAMs for $GABA_AR$s (Figure 4e). Among the other six PAM candidates (43 (AA-861), 225 (CGP-7930), 226 (CGP-13501), 419 (Retro-2), 1254 (vinpocetine), and 1275 (YC-1)), CGP-7930 and CGP-13501 have been reported to be PAMs for $GABA_B$ receptors ($GABA_BR$s).[40] AA-861, Retro-2, vinpocetine, and YC-1 have been characterized as a 5-lipooxgenase inhibitor,[41] an endosome-to-Golgi retrograde transport inhibitor,[42] a phosphodiesterase-1 inhibitor,[43] and a guanylate cyclase activator,[44] respectively. To our knowledge, there have been no reports pertaining to the affinity of these six compounds for $GABA_AR$s. Six compounds were assigned as potential orthosteric ligands by the fourth screening (Figure 4c,d), four of which were known antagonists or inhibitors for $GABA_AR$s (605 (hydrastine), 680 (thiocolchicine), 1066 (reactive blue-2), and 1132 (gabazine)) and two were new ligands (991 (K-114) and 1070 (daurisoline)) as shown in Figure 4d. K-114 and daurisoline have been reported as an amyloid fiber staining dye[45] and a hERG K^+ channel blocker, respectively. No previous reports have been found that described the interaction of these compounds with $GABA_AR$s.

Characterization of Hit Compounds. We subsequently characterized in detail the binding properties of the newly discovered $GABA_AR$ ligand candidates by the fluorescence assay using Gzn-OG and electrophysiological measurements (except for AA-861, which was not commercially available). As shown in Figure 5a, it was clearly confirmed that the affinity of GABA to $GABA_AR(\alpha1/\beta3/\gamma2)$ was largely enhanced in the presence of these PAM candidates (25 μM concentrations of CGP-7930, CGP-13501, vinpocetine, Retro-2, or YC-1). The K_d values of GABA were determined from the concentration−response curves to be 0.095, 0.38, 0.26, 0.46, and 0.21 μM in the presence of CGP-7930, CGP-13501, vinpocetine, Retro-2, and YC-1, respectively. The affinities of these compounds to the $GABA_AR$ were also determined from the fluorescence titration curves at a fixed GABA concentration (10 μM): K_d = 13.1, 14.4, 1.4, 4.7, and 6.8 μM for CGP-7930, CGP-13501, vinpocetine, Retro-2, and YC-1, respectively (Figure S16a). Addition of the orthosteric ligands daurisoline and K-114 caused a significant decrease in the fluorescence intensity at the cell surface in the absence of GABA in a concentration-dependent manner, with K_d values of 2.2 and 5.8 μM for daurisoline and K-114, respectively (Figure S16b).

To validate the impact of these hit compounds on $GABA_AR$ functions, we finally examined the ion-channel activity of $GABA_AR$s by patch-clamp electrophysiological assays. At high concentrations (100 μM for CGP-7930 and CGP-13501, and 25 μM for vinpocetine, Retro-2, and YC-1), all of these compounds increased the chloride currents in HEK293T cells expressing $GABA_AR(\alpha1/\beta3/\gamma2)$, even in the absence of GABA, indicating that these compounds acted as allosteric agonists as well as PAMs (Figure S17a,b). Similar behavior has been reported for well-known $GABA_AR$ PAMs, including barbiturates, propofol, and etomidate at high concentrations.[46,47] On the other hand, at low concentrations, vinpocetine, Retro-2 and YC-1 did not induce any direct activation of $GABA_AR$s (Figure S17b), and the GABA-induced chloride currents were reversibly enhanced by these compounds as shown in Figure 5b. The EC_{50} values of GABA in the presence of 3 μM of each compound were electrophysiologically determined to be 13.7, 4.8, and 2.8 μM with vinpocetine, Retro-2, and YC-1, respectively (Figure 5c). The K_d values of GABA determined by our fluorescent assay using Gzn-OG were 1.8, 6.7, and 3.9 μM with vinpocetine, Retro-2, and YC-1, respectively under the same conditions (Figure S18). These K_d values for Retro-2 and YC-1 were almost identical to those obtained from the electrophysiological assays, while the value for vinpocetine was different between the two assay systems. This result may be attributed to the fact that vinpocetine interacts with $GABA_AR$s as a PAM in a more complicated manner than Retro-2 or YC-1.

DISCUSSION

The impact of small molecules on $GABA_AR$ functions can be evaluated by the patch-clamp electrophysiological assay, a powerful and standard technique having high sensitivity. However, application of the patch-clamp method for drug screening is often limited because of its low-throughput properties. Membrane potential assays using voltage-sensitive dyes can be used as alternatives to the patch-clamp assay for high-throughput screening.[48,49] Although useful, some of the dyes used in these methods directly modulate the ion-channel properties of $GABA_AR$s, which results in detection of many false positive compounds.[50] Semisynthetic protein-based biosensors are attractive tools for exploring the direct binding of compounds to membrane receptors. In a successful example of such biosensors, Johnsson and co-workers constructed $GABA_B$ receptor ($GABA_BR$)-based semisynthetic biosensors as a proof-of-principle. This method was used to detect allosteric modulators, as well as orthosteric ligands, using a Snifits (SNAP-tag based indicator with a fluorescent intramolecular tether) technique.[51,52] Although powerful, these approaches usually require the fusion of relatively large protein tags (such as SNAP-, CLIP-, or GFP-tags) to the target receptors. Given the delicate oligomeric structures of complicated membrane receptors, such as ion-channel-type $GABA_AR$s (which exist as heteropentameric complexes), it would be difficult to apply these protein-based semisynthetic strategies to these proteins. We have previously reported the construction of $GABA_AR$-based biosensors by a combination of LDAI-based chemical labeling and a BFQR method.[23] However, this method requires long incubation periods for the chemical labeling (3−4 h) followed by washing operations (three times) and requires addition of a newly synthesized quencher-ligand conjugate for preparation of the FRET sensor, which is not very suitable for high-throughput drug screening (Figure S19).

DOI: 10.1021/acscentsci.9b00539
ACS Cent. Sci. 2019, 5, 1541−1553

Recently, turn-on fluorescent probes have received considerable attention as tools for molecular imaging because of the simple protocols involved.[53] However, application of these probes to the quantitative analysis of ligand−protein interactions and drug screening has been limited to date. Here, we developed a turn-on fluorescent probe (Gzn-OG) for $GABA_A$Rs, by which a fluorescent biosensor was constructed in a quick and effective manner. Indeed, simple addition of the probe to the culture medium allowed the analysis of ligand−protein interactions and high-throughput screening of small molecules to determine orthosteric ligands and PAMs of $GABA_A$Rs under live cell conditions. To the best of our knowledge, this is the first report of a ligand assay system exploiting a turn-on imaging probe for ion-channel receptors, which are important drug targets.

Because the rational design of allosteric modulators is much more difficult compared with orthosteric or competitive ligands, it is desirable to develop efficient drug discovery platforms for allosteric modulators from screening. We have previously identified four compounds from the LOPAC1280 library, using our cell-based biosensors constructed by LDAI labeling and using the BFQR method, as benzodiazepine ligands (see also Figure S1).[23] However, this system was specialized for identifying competitive ligands at the benzodiazepine site. We actually attempted to construct a biosensor by a combination of LDAI and BFQR methods using CGAM-Gzn and Gzn-Q; however, the fluorescence change by the addition of etomidate (200 μM) in the presence of GABA (30 μM) was too small to detect etomidate, possibly due to the low labeling efficiency and the less sufficient quenching/recovery of fluorescence (Figure S20). Given many allosteric sites exist in the $GABA_A$R scaffolds, more versatile biosensors that can detect any type of allosteric modulator are desirable. The present biosensor developed by exploiting the affinity modulation of GABA in the presence of PAMs should be a rational platform capable of detecting PAMs of $GABA_A$Rs, and indeed we identified not only six orthosteric ligands but also 13 PAMs. These hit compounds included four known orthosteric inhibitors and seven known PAMs. It is worth noting that most of the known PAMs for $GABA_A$Rs included in the LOPAC1280 library were detected by the present screening assay (seven of eight known PAMs), clearly validating the feasibility of our biosensor system using Gzn-OG.

We here discovered eight new ligands (two competitive ligands and six PAMs) for $GABA_A$Rs. Among the newly found PAMs, CGP-7930 and CGP-13501 are structural analogues of propofol, which suggests these compounds may bind to the propofol-binding site in $GABA_A$Rs. In contrast, the other compounds may bind to unknown sites because the molecular structures of these compounds do not resemble any already known $GABA_A$R ligands. In particular, YC-1 and Retro-2 that induced large shifts in the dose-dependency of GABA in the electrophysiological assay may be potentially new types of allosteric modulators for $GABA_A$Rs, although careful examination of the mechanisms of action will be required in combination with other methods to confirm this. With respect to YC-1, there is a report on a potent neuroprotective activity against the glutamate-induced excitotoxicity in cultured neurons, although the detailed mechanism still remains unclear.[54] The positive allosteric modulation of $GABA_A$Rs by YC-1 may potentially be involved in the neuroprotective effect on cultured neurons. Since $GABA_A$Rs mainly mediate the fast inhibitory neurotransmission in the central nervous system (CNS), the functions are deeply associated with all aspects of brain functions. The new discovery of PAMs for $GABA_A$Rs may contribute to the elucidation of the $GABA_A$R related neuroregulatory mechanisms in CNS.

In conclusion, our biosensor system using the fluorescent turn-on Gzn-OG probe demonstrated the capacity to discover new allosteric ligands acting on an unknown binding site of $GABA_A$R. Also, this method clearly highlighted the power of turn-on fluorescent probes to screen for drugs acting on complicated membrane proteins that cannot be investigated by conventional methods.

MATERIALS AND METHODS

Synthesis. All synthesis procedures and characterizations are described in the Supporting Information.

Expression of $GABA_A$Rs in HEK293T Cells. HEK293T cells (ATCC) were cultured in Dulbecco's modified Eagle's medium (DMEM) supplemented with 10% fetal bovine serum (Sigma-Aldrich), penicillin (100 units mL^{-1}), streptomycin (100 μg mL^{-1}), and amphotericin B (250 ng mL^{-1}) and incubated in a 5% CO_2 humidified chamber at 37 °C. For expression of $GABA_A$R, HEK293T cells (3.0×10^5 cells) plated on a 6 cm dish (Corning) were transfected with each expression vector for α, β, and γ subunits (pCAGGS(α1 $GABA_A$R), pCAGGS(β3 $GABA_A$R), and pCAGGS(γ2 $GABA_A$R)) and pmCherry-F or pEGFP-F as a transfection marker using Lipofectamine 2000 (Invitrogen) according to the manufacture's instructions.

Confocal Live Imaging of HEK293T Cells Stained with an Imaging Probe. After 24 h of transfection, the cells were dissociated by treating with 0.05% trypsin/EDTA and reseeded on 35 mm glass-bottom dishes (Matsunami) pretreated with poly-L-lysine. After 24 h of the reseeding, the cells were washed twice with HBS (20 mM HEPES, 107 mM NaCl, 6 mM KCl, 2 mM $CaCl_2$ and 1.2 mM $MgSO_4$ and 11.5 mM glucose at pH 7.4), and then 1 mL of HBS containing an imaging probe was added into the cell cultured dish. Fluorescence imaging of the cells was performed using a confocal laser scanning microscopy (Carl Zeiss, LSM-800) equipped with a 63×, NA = 1.40 oil objective, and a GaAsP detector. Fluorescence images were acquired using the 405 nm excitation for DBD; the 488 nm excitation for OG, Fl, Alexa Fluor 488, EGFP-F; the 561 nm excitation for mCherry-F; the 640 nm excitaion for Alexa Fluor 647 derived from diode lasers with control of the focus using the Definite Focus module (Carl Zeiss).

UV−vis Spectra Measurements. UV−vis spectra were measured on a Shimadzu UV-2600 spectrophotometer using a quartz cell with 1.0 cm path length at r.t. The compound was dissolved in HBS buffer (pH7.4).

Fluorescence Spectra Measurements. Fluorescence spectra were measured on a PerkinElmer LS55 fluorescence spectrometer using a quartz cell with 0.1 × 1.0 cm path length at an excitation wavelength of 430 nm (for DBD), 496 nm (for Fl, OG, and Ax488), and 650 nm (for Ax647) at r.t. The compound was dissolved in HBS buffer.

Determination of the Dissociation Constant of Gzn-OG for $GABA_A$Rs on Live Cells. The HEK293T cells transiently transfected with $GABA_A$R(α1/β3/γ2) on a 35 mm glass-bottom dish were washed twice with HBS, and then 2 mL of HBS containing 8 μM Gzn-OG was added into the cell cultured dish. The 2-fold serial dilutions of Gzn-OG were conducted, and the CLSM image was observed at each Gzn-OG concentration. The fluorescence intensities (F) of plasma

DOI: 10.1021/acscentsci.9b00539
ACS Cent. Sci. 2019, 5, 1541−1553

membranes of cells were determined by line plot analyses of the CLSM images. The same points were monitored during the measurements, and the values were averaged. The dissociation constant (K_d(Gzn-OG)) was determined by fitting with the theoretical logistic equation.

$$\Delta F/\Delta F_{max} = 1/[1 + (\log[\text{Gzn-OG}]/\log K_d(\text{Gzn-OG}))^n]$$

$$\Delta F = F - F_{min}$$

$$\Delta F_{max} = F_{max} - F_{min}$$

$$\log n = h$$

where F_{min} and F_{max} are theoretically determined minimum and maximum fluorescence intensities, respectively. h is a Hill's coefficient.

Determination of the Dissociation Constants of Orthosteric Ligands on Live Cells Using Gzn-OG. The concentration of Gzn-OG was fixed at 100 nM in each experiment. After the HEK293T cells transfected with $GABA_AR(\alpha1/\beta3/\gamma2)$ were washed on a 35 mm glass-bottom dish with HBS (1 mL × 2), 100 nM Gzn-OG dissolved in HBS (1 mL) was added into the cell cultured dish. Thereafter, a stock solution of each orthosteric ligand containing 100 nM Gzn-OG was applied to the cell cultured dish, and the CLSM imaging was performed without any washing operations. The fluorescence intensity (F) of the plasma membrane of a single cell at each ligand concentration was determined by enclosing the regions containing a cell with ROIs and F/F_0 value was calculated for each cell (F_0 is a fluorescence intensity in the absence of ligand). For removing the contribution of background fluorescence, the averaged background intensity was subtracted from F and F_0. After the averaged F/F_0 values were plotted against ligand concentrations, the dissociation constant of each ligand was determined by fitting with the theoretical logistic equation.

$$F/F_0 = 1 - 1/(1 + (\log[\text{ligand}]/\log K_d(\text{ligand}))^n)$$

$$\log n = h$$

where F and F_0 are a fluorescence intensity at each ligand concentration and that in the absence of ligand. h is a Hill's coefficient.

Method for the Detection of Ligand for $GABA_AR$ using Gzn-OG. The concentrations of Gzn-OG (100 nM) and GABA (10 or 0 μM) was fixed in each experiment. After adding of Gzn-OG to the HEK293T cells transfected with $GABA_AR(\alpha1/\beta3/\gamma2)$, a stock solution of each compound containing Gzn-OG (100 nM) and GABA (10 or 0 μM) was applied to the cell cultured dish and CLSM imaging was performed without any washing operations. The fluorescence intensities of plasma membranes of cells in the presence or absence of each compound were determined by enclosing the regions containing a single cell with ROIs. The fluorescence change ratio ($\Delta F/F_0$) was calculated for each single cell and averaged. The $\Delta F/F_0$ was defined by a following equation.

$$\Delta F/F_0 = (F - F_0)/F_0$$

where F and F_0 are fluorescence intensities in the presence and absence of each ligand.

Determination of the Dissociation Constants of GABA in the Presence and Absence of a PAM. The concentrations of Gzn-OG (100 nM) and an allosteric modulator (propofol 200 μM; etomidate 200 μM; zolpidem 20 μM) were fixed in each experiment. After adding of Gzn-OG and a ligand to the HEK293T cells transfected with $GABA_AR(\alpha1/\beta3/\gamma2)$, a stock solution of GABA containing Gzn-OG (100 nM) and each PAM was applied to the cell cultured dish and CLSM imaging was performed without any washing operations. The fluorescence intensity (F) of the plasma membrane was determined as described in Determination of the Dissociation Constant of Gzn-OG. After plotting of the averaged F/F_0 values against GABA concentrations, the EC_{50}(GABA) and dissociation constant (K_d(GABA)) were determined by fitting with the theoretical logistic equation.

$$F/F_0 = 1 - 1/(1 + (\log[\text{GABA}]/EC_{50}(\text{GABA}))^n)$$

$$\log n = h$$

$$K_d(\text{GABA}) = EC_{50}(\text{GABA}) \times K_d(\text{Gzn-OG})/([\text{Gzn-OG}] + K_d(\text{Gzn-OG}))$$

where F and F_0 are a fluorescence intensity at each GABA concentration and that in the absence of GABA. h is a Hill's coefficient.

Determination of the Dissociation Constants of PAM for $GABA_AR$. The concentrations of Gzn-OG (100 nM) and GABA (10 μM) were fixed in each experiment. After adding of Gzn-OG and GABA to the HEK293T cells transfected with $GABA_AR(\alpha1/\beta3/\gamma2)$, a stock solution of each PAM containing Gzn-OG (100 nM) and GABA (10 μM) was applied to the cell cultured dish, and CLSM imaging was performed without any washing operations. The fluorescence intensity (F) of the plasma membrane was determined as described in Determination of the Dissociation Constant of Gzn-OG. After plotting of the averaged F/F_0 values against PAM concentrations, the dissociation constant (K_d(PAM)) was determined by fitting with the theoretical logistic equation.

$$F/F_0 = 1 - 1/(1 + (\log[\text{PAM}]/K_d(\text{PAM}))^n)$$

$$\log n = h$$

where F and F_0 are a fluorescence intensity at each PAM concentration and that in the absence of PAM. h is a Hill's coefficient.

High-Throughput Screening of PAMs on $GABA_AR$ Using Gzn-OG. The concentrations of Gzn-OG and GABA were fixed at 100 nM and 10 μM, respectively. A library of pharmacologically active compounds (the LOPAC1280 (Sigma-Aldrich)) was employed in this screening assay. To enhance the screening efficiency, ligand screening was performed in three different steps. In addition, an additional screening was conducted in the last step to detect the compounds competitively bind to the orthosteric site. In the first screening, 7−8 individual compounds (1.5 μL × 10 mM each compound in DMSO) were mixed in the same tube and evaporated to remove DMSO. Then, the residue was redissolved in 1.5 μL of DMSO and diluted with 500 μL of HBS containing Gzn-OG (100 nM) and GABA (10 μM). The solution was added to the $GABA_AR(\alpha1/\beta3/\gamma2)$-transfected cells in 1 mL of HBS containing Gzn-OG (100 nM) and GABA (10 μM) (final concentration of each compound was 10 μM). After 1 min incubation, CLSM imaging was performed without any washing operations. The fluorescence intensities before and after addition of a compounds mixture were determined by enclosing the regions containing a cell with ROIs. The fluorescence change ratio ($-\Delta F/F_0$) was calculated

DOI: 10.1021/acscentsci.9b00539
ACS Cent. Sci. 2019, 5, 1541−1553

for a single cell and averaged. (Data represent mean ± SEM n = 7−12) ($\Delta F = F - F_0$, where F and F_0 were fluorescence intensities before and after addition of compounds mixture, respectively). Threshold value of the $-\Delta F/F_0$ ratio was defined as 0.5. In this step, compounds showing intrinsic fluorescence were excluded in the assay. In the second screening, each hit group in the first screening was divided into two subgroups containing four compounds. Four compounds (1.5 μL × 10 mM each compound in DMSO) were mixed in each subgroup. The mixture was added to a Gzn-OG assay system (final concentration of each compound was 10 μM), and the $-\Delta F/F_0$ ratio was calculated for a single cell and averaged (data represent mean ± SEM n = 8−12). Threshold value of the $-\Delta F/F_0$ ratio was defined as 0.4. In the third screening, the cells stained with Gzn-OG (100 nM) were treated with each compound (final concentration of each compound was 10 μM) in the presence of 10 μM GABA, and the averaged $-\Delta F/F_0$ ratio was determined (data represent mean ± SEM n = 10−12). Threshold value of the $-\Delta F/F_0$ ratio in the third screening was defined as 0.3. In the last screening assay, each hit compound in the third screening assay was applied to the cell cultured dish containing Gzn-OG (100 nM) in the absence of GABA. The compounds exhibiting the $-\Delta F/F_0$ ratio > 0.3 were identified as orthosteric ligands for $GABA_AR(\alpha1/\beta3/\gamma2)$ (data represent mean ± SEM n = 10−12).

Electrophysiology. For electrophysiological measurements, coverslips with HEK293T cells transfected with $GABA_AR(\alpha1/\beta3/\gamma2)$ were placed in the experimental chamber. Membrane currents were recorded at room temperature (25 °C) in the whole-cell mode of a patch-clamp technique with an Axopatch 200B (Molecular devices) patch-clamp amplifier. Patch electrodes having a resistance of 2−5 MΩ (with internal solution) were fabricated from borosilicate glass capillaries using a P-97 pipet puller (Sutter Instrument). Current signals were filtered at 5 kHz with a 4-pole Bessel filter and digitized at 20 kHz. The pCLAMP (version 10.5.1.0; Molecular devices) software was used for command pulse control, data acquisition, and analysis. For whole-cell recording, the series resistance was compensated (to 70−80%) to minimize voltage errors. The extracellular solution contained (in mM): 140 NaCl, 5 KCl, 2 $CaCl_2$, 1 $MgCl_2$, 10 glucose, and 10 HEPES (pH adjusted to 7.4 with NaOH, and osmolality adjusted to 300 mmol kg^{-1} with D-mannitol). Intracellular solutions contained (in mM): 55 K gluconate, 50 KCl, 26 NaCl, 0.5 $CaCl_2$, 3 $MgCl_2$, 2 Na_2ATP, 5 EGTA, 5 HEPES, and 5 creatine-phosphate (pH 7.2 adjusted with KOH, and osmolality adjusted to 290 mmol kg^{-1} with D-mannitol). Relative current (I) in Supplementary Figure 17b was defined by the following equation; relative $I = I_A/I_{Ctl}$, where I_{Ctl} and I_A are the peak amplitudes of whole-cell currents observed before and after a hit compound application, respectively. In Figure 5b, GABA concentration−response curves were fitted to the logistic equation: $I = (A_{max} - A_0)/[1 + (X/EC_{50})n] + A_0$, where I is current amplitude, A_{max} and A_0 are the maximum and minimum values of the measured parameter, X is GABA concentration; n is a Hill coefficient; EC_{50} is the concentration of GABA that generates half-maximal amplitude. Data points in figures represent the means of n individual measurements from different cells.

■ ASSOCIATED CONTENT

Supporting Information

The Supporting Information is available free of charge on the ACS Publications website at DOI: 10.1021/acscentsci.9b00539.

Additional data referenced in the text (Figures S1−S20); general materials and methods for organic synthesis; and an additional reference (PDF)

Compounds data included in LOPAC1280 (XLSX)

Screening data (XLSX)

■ AUTHOR INFORMATION

Corresponding Author

*E-mail: ihamachi@sbchem.kyoto-u.ac.jp.

ORCID

Seiji Sakamoto: 0000-0002-0605-0987

Itaru Hamachi: 0000-0002-3327-3916

Present Addresses

⊥(K.Y.) Department of Molecular Imaging and Theranostics, National Institute of Radiological Sciences, QST, Anagawa 4-9-1, Inage-ku, Chiba 263-8555, Japan.

#(S.K.) Department of Biomolecular Engineering, Graduate School of Engineering, Nagoya University, Furo-cho, Chikusa-ku, Nagoya 464−8603, Japan.

Notes

The authors declare no competing financial interest.

■ ACKNOWLEDGMENTS

This work was funded by a Grant-in-Aid for Scientific Research on Innovative Areas "Chemistry for Multimolecular Crowding Biosystems" (JSPS KAKENHI Grant No. 17H06348) to I.H., a Grant-in-Aid for Scientific Research (B) (JSPS KAKENHI Grant No. 16H03290) to S.K., Daiichi Sankyo Foundation of Life Science to S.K., and the Takeda Science Foundation to S.K., and supported by JST ERATO Grant Number JPMJER1802 to I.H. and S.K.

■ REFERENCES

(1) Christopoulos, A. Allosteric Binding Sites on Cell-Surface Receptors: Novel Targets for Drug Discovery. *Nat. Rev. Drug Discovery* **2002**, *1*, 198−210.

(2) Conn, P. J.; Lindsley, C. W.; Meiler, J.; Niswender, C. M. Opportunities and Challenges in the Discovery of Allosteric Modulators of GPCRs for Treating CNS Disorders. *Nat. Rev. Drug Discovery* **2014**, *13*, 692−708.

(3) Lu, S.; Li, S.; Zhang, J. Harnessing Allostery: a Novel Approach to Drug Discovery. *Med. Res. Rev.* **2014**, *34*, 1242−1285.

(4) Ludlow, R. F.; Verdonk, M. L.; Saini, H. K.; Tickle, I. J.; Jhoti, H. Detection of Secondary Binding Sites in Proteins using Fragment Screening. *Proc. Natl. Acad. Sci. U. S. A.* **2015**, *112*, 15910−15915.

(5) Prasannan, C. B.; Villar, M. T.; Artigues, A.; Fenton, A. W. Identification of Regions of Rabbit Muscle Pyruvate Kinase Important for Allosteric Regulation by Phenylalanine, Detected by H/D Exchange Mass Spectrometry. *Biochemistry* **2013**, *52*, 1998−2006.

(6) Maurer, T.; Garrenton, L. S.; Oh, A.; Pitts, K.; Anderson, D. J.; Skelton, N. J.; Fauber, B. P.; Pan, B.; Malek, S.; Stokoe, D.; Ludlam, M. J. C.; Bowman, K. K.; Wu, J.; Giannetti, A. M.; Starovasnik, M. A.; Mellman, I.; Jackson, P. K.; Rudolph, J.; Wang, W.; Fang, G. Small-Molecule Ligands Bind to a Distinct Pocket in Ras and Inhibit SOS-Mediated Nucleotide Exchange Activity. *Proc. Natl. Acad. Sci. U. S. A.* **2012**, *109*, 5299−5304.

(7) Lazareno, S.; Gharagozloo, P.; Kuonen, D.; Popham, A.; Birdsall, N. J. M. Subtype-Selective Positive Cooperative Interactions between

DOI: 10.1021/acscentsci.9b00539
ACS Cent. Sci. 2019, 5, 1541−1553

Brucine Analogues and Acetylcholine at Muscarinic Receptors: Radioligand Binding Studies. *Mol. Pharmacol.* **1998**, *53*, 573−589.
(8) Leach, K.; Sexton, P. M.; Christopoulos, A. Quantification of Allosteric Interactions at G Protein Coupled Receptors Using Radioligand Binding Assays. *Curr. Protoc. Pharmacol.* **2011**, *52*, 1−22.
(9) Hulme, E. C.; Trevethick, M. A. Ligand Binding Assays at Equilibrium: Validation and Interpretation. *Br. J. Pharmacol.* **2010**, *161*, 1219−1237.
(10) Rudolph, U.; Knoflach, F. Beyond Classical Benzodiazepines: Novel Therapeutic Potential of $GABA_A$ Receptor Subtypes. *Nat. Rev. Drug Discovery* **2011**, *10*, 685−697.
(11) Dineley, K. T.; Pandya, A. A.; Yakel, J. L. Nicotinic ACh Receptors as Therapeutic Targets in CNS Disorders. *Trends Pharmacol. Sci.* **2015**, *36*, 96−108.
(12) Nutt, D. J.; Malizia, A. New Insights into the Role of the $GABA_A$-Benzodiazepine Receptor in Psychiatric Disorder. *Br. J. Psychiatry* **2001**, *179*, 390−396.
(13) Chebib, M.; Johnston, G. A. R. GABA-Activated Ligand Gated Ion Channels: Medicinal Chemistry and Molecular Biology. *J. Med. Chem.* **2000**, *43*, 1427−1447.
(14) Sieghart, W. Allosteric Modulation of $GABA_A$ Receptors *via* Multiple Drug-Binding Sites. *Adv. Pharmacol.* **2015**, *72*, 53−96.
(15) Sigel, E.; Buhr, A. The Benzodiazepine Binding Site of $GABA_A$ Receptors. *Trends Pharmacol. Sci.* **1997**, *18*, 425−429.
(16) Sieghart, W. Structure and Pharmacology of γ-Aminobutyric $Acid_A$ Receptor Subtypes. *Pharmacol. Rev.* **1995**, *47*, 181−234.
(17) Bateson, A. N. Basic Pharmacologic Mechanisms Involved in Benzodiazepine Tolerance and Withdrawal. *Curr. Pharm. Des.* **2002**, *8*, 5−21.
(18) Tan, K. R.; Brown, M.; Labouèbe, G.; Yvon, C.; Creton, C.; Fritschy, J.-M.; Rudolph, U.; Lüscher, C. Neural Bases for Addictive Properties of Benzodiazepines. *Nature* **2010**, *463*, 769−774.
(19) Tan, K. R.; Rudolph, U.; Lüscher, C. Hooked on Benzodiazepines: $GABA_A$ Receptor Subtypes and Addiction. *Trends Neurosci.* **2011**, *34*, 188−197.
(20) Jacob, T. C.; Michels, G.; Silayeva, L.; Haydon, J.; Succol, F.; Moss, S. J. Benzodiazepine Treatment Induces Subtype-Specific Changes in $GABA_A$ Receptor Trafficking and Decreases Synaptic Inhibition. *Proc. Natl. Acad. Sci. U. S. A.* **2012**, *109*, 18595−18600.
(21) Soyka, M. Treatment of Benzodiazepine Dependence. *N. Engl. J. Med.* **2017**, *376*, 1147−1157.
(22) Bachhuber, M. A.; Hennessy, S.; Cunningham, C. O.; Starrels, J. L. Increasing Benzodiazepine Prescriptions and Overdose Mortality in the United States, 1996−2013. *Am. J. Public Health* **2016**, *106*, 686−688.
(23) Yamaura, K.; Kiyonaka, S.; Numata, T.; Inoue, R.; Hamachi, I. Discovery of Allosteric Modulators for $GABA_A$ Receptors by Ligand-Directed Chemistry. *Nat. Chem. Biol.* **2016**, *12*, 822−830.
(24) Fujishima, S.-H.; Yasui, R.; Miki, T.; Ojida, A.; Hamachi, I. Ligand-Directed Acyl Imidazole Chemistry for Labeling of Membrane-Bound Proteins on Live Cells. *J. Am. Chem. Soc.* **2012**, *134*, 3961−3964.
(25) Wang, H.; Koshi, Y.; Minato, D.; Nonaka, H.; Kiyonaka, S.; Mori, Y.; Tsukiji, S.; Hamachi, I. Chemical Cell-Surface Receptor Engineering Using Affinity-Guided, Multivalent Organocatalysts. *J. Am. Chem. Soc.* **2011**, *133*, 12220−12228.
(26) Zhuang, Y.-D.; Chiang, P.-Y.; Wang, C.-W.; Tan, K.-T. Environment-Sensitive Turn-on Probes Targeting Hydrophobic Ligand-Binding Domains for Selective Protein Detection. *Angew. Chem., Int. Ed.* **2013**, *52*, 8124−8128.
(27) Mortensen, M.; Iqbal, F.; Pandurangan, A. P.; Hannan, S.; Huckvale, R.; Topf, M.; Baker, J. R.; Smart, T. G. Photo-Antagonism of the $GABA_A$Receptor. *Nat. Commun.* **2014**, *5*, 4454.
(28) Iqbal, F.; Ellwood, R.; Mortensen, M.; Smart, T. G.; Baker, J. R. Synthesis and Evaluation of Highly Potent $GABA_A$Receptor Antagonists Based on Gabazine (SR-95531). *Bioorg. Med. Chem. Lett.* **2011**, *21*, 4252−4254.
(29) Slany, A.; Zezula, J.; Tretter, V.; Sieghart, W. Rat β3 Subunits Expressed in Human Embryonic Kidney 293 Cells Form High Affinity [35S] t-Butylbicyclophosphorothionate Binding Sites Modulated by Several Allosteric Ligands of Gamma-Aminobutyric Acid Type A Receptors. *Mol. Pharmacol.* **1995**, *48*, 385−391.
(30) Davies, P. A.; Kirkness, E. F.; Hales, T. G. Modulation by General Anaesthetics of Rat $GABA_A$ Receptors Comprised of $\alpha1\beta3$ and $\beta3$ Subunits Expressed in Human Embryonic Kidney 293 Cells. *Br. J. Pharmacol.* **1997**, *120*, 899−909.
(31) Hanson, S. M.; Czajkowski, C. Structural Mechanism Underlying Benzodiazepine Modulation of the $GABA_A$ Receptor. *J. Neurosci.* **2008**, *28*, 3490−3499.
(32) Wafford, K. A.; Whiting, P. J.; Kemp, J. A. Differences in Affinity and Efficacy of Benzodiazepine Receptor Ligands at Recombinant γ-Aminobutyric $Acid_A$ Receptor subtypes. *Mol. Pharmacol.* **1993**, *43*, 240−244.
(33) Olsen, R. W. $GABA_A$ receptor: Positive and Negative Allosteric Modulators. *Neuropharmacology* **2018**, *136*, 10−22.
(34) Feng, H.-J.; Jounaidi, Y.; Haburcak, M.; Yang, X.; Forman, S. A. Etomidate Produces Similar Allosteric Modulation in $\alpha1\beta3\delta$ and $\alpha1\beta3\gamma2L$ $GABA_A$ Receptors. *Br. J. Pharmacol.* **2014**, *171*, 789−798.
(35) Akk, G.; Shin, D. J.; Germann, A. L.; Steinbach, J. H. GABA Type A Receptor Activation in the Allosteric Coagonist Model Framework: Relationship between EC_{50} and Basal Activity. *Mol. Pharmacol.* **2018**, *93*, 90−100.
(36) Has, A. T. C.; Absalom, N.; van Nieuwenhuijzen, P. S.; Clarkson, A. N.; Ahring, P. K.; Chebib, M. Zolpidem Is a Potent Stoichiometry-Selective Modulator of $\alpha1\beta3$ $GABA_A$ Receptors: Evidence of a Novel Benzodiazepine Site in $\alpha1-\alpha1$ Interface. *Sci. Rep.* **2016**, *6*, 28674.
(37) Pejo, E.; Santer, P.; Wang, L.; Dershwitz, P.; Husain, S. S.; Raines, D. E. γ-Aminobutyric Acid Type A Receptor Modulation by Etomidate Analogs. *Anesthesiology* **2016**, *124*, 651−663.
(38) Lingamaneni, R.; Krasowski, M. D.; Jenkins, A.; Truong, T.; Giunta, A. L.; Blackbeer, J.; MacIver, M. B.; Harrison, N. L.; Hemmings, H. C., Jr. Anesthetic Properties of 4-Iodopropofol: Implications for Mechanisms of Anesthesia. *Anesthesiology* **2001**, *94*, 1050−1057.
(39) Zhang, J.-H.; Chung, T. D. Y.; Oldenburg, K. R. A Simple Statistical Parameter for Use in Evaluation and Validation of High Throughput Screening Assays. *J. Biomol. Screening* **1999**, *4*, 67−73.
(40) Urwyler, S.; Mosbacher, J.; Lingenhoehl, K.; Heid, J.; Hofstetter, K.; Froestl, W.; Bettler, B.; Kaupmann, K. Positive Allosteric Modulation of Native and Recombinant γ-Aminobutyric $Acid_B$Receptors by 2,6-Di-tert-butyl-4-(3-hydroxy-2,2-dimethyl-propyl)-phenol (CGP7930) and Its Aldehyde Analog CGP13501. *Mol. Pharmacol.* **2001**, *60*, 963−971.
(41) Mita, H.; Yui, Y.; Shida, T. Effect of AA-861, a 5-Lipoxygenase Inhibitor, on Leukotriene Synthesis in Human Polymorphonuclear Leukocytes and on Cyclooxygenase and 12-Lipoxygenase Activities in Human Platelets. *Allergy* **1986**, *41*, 493−498.
(42) Sivan, G.; Weisberg, A. S.; Americo, J. L.; Moss, B. Retrograde Transport from Early Endosomes to the Trans-Golgi Network Enables Membrane Wrapping and Egress of Vaccinia Virus Virions. *J. Virol.* **2016**, *90*, 8891−8905.
(43) Hagiwara, M.; Endo, T.; Hidaka, H. Effects of Vinpocetine on Cyclic Nucleoside Metabolism in Vascular Smooth Muscle. *Biochem. Pharmacol.* **1984**, *33*, 453−457.
(44) Ko, F.-N.; Wu, C.-C.; Kuo, S.-C.; Lee, F.-Y.; Teng, C.-M. YC-1, A Novel Activator of Platelet Guanylate Cyclase. *Blood* **1994**, *84*, 4226−4233.
(45) Crystal, A. S.; Giasson, B. I.; Crowe, A.; Kung, M.-P.; Zhuang, Z.-P.; Trojanowski, J. Q.; Lee, V. M.-Y. A Comparison of Amyloid Fibrillogenesis Using the Novel Fluorescent Compound K114. *J. Neurochem.* **2003**, *86*, 1359−1368.
(46) Hill-Venning, C.; Belelli, D.; Peters, J. A.; Lambert, J. J. Subunit-Dependent Interaction of the General Anaesthetic Etomidate with the γ-Aminobutyric Acid Type A Receptor. *Br. J. Pharmacol.* **1997**, *120*, 749−756.

DOI: 10.1021/acscentsci.9b00539
ACS Cent. Sci. 2019, 5, 1541−1553

(47) Franks, N. P. General Anaesthesia: from Molecular Targets to Neuronal Pathways of Sleep and Arousal. *Nat. Rev. Neurosci.* **2008**, *9*, 370−386.
(48) Fairless, R.; Beck, A.; Kravchenko, M.; Williams, S. K.; Wissenbach, U.; Diem, R.; Cavalié, A. Membrane Potential Measurements of Isolated NeuronsUsing a Voltage-Sensitive Dye. *PLoS One* **2013**, *8*, No. e58260.
(49) Joesch, C.; Guevarra, E.; Parel, S. P.; Bergner, A.; Zbinden, P.; Konrad, D.; Albrecht, H. Use of FLIPR Membrane Potential Dyes for Validation of High-Throughput Screening with the FLIPR and UARCS Technologies: Identification of Ion Channel Modulators Acting on the $GABA_A$Receptor. *J. Biomol. Screening* **2008**, *13*, 218−228.
(50) Mennerick, S.; Chisari, M.; Shu, H.-J.; Taylor, A.; Vasek, M.; Eisenman, L. N.; Zorumski, C. F. Diverse Voltage-Sensitive Dyes Modulate $GABA_A$Receptor Function. *J. Neurosci.* **2010**, *30*, 2871−2879.
(51) Brun, M. A.; Tan, K.-T.; Griss, R.; Kielkowska, A.; Reymond, L.; Johnsson, K. A. Semisynthetic Fluorescent Sensor Protein for Glutamate. *J. Am. Chem. Soc.* **2012**, *134*, 7676−7678.
(52) Masharina, A.; Reymond, L.; Maurel, D.; Umezawa, K.; Johnsson, K. A Fluorescent Sensor for GABA and Synthetic $GABA_B$ Receptor Ligands. *J. Am. Chem. Soc.* **2012**, *134*, 19026−19034.
(53) Klymchenko, A. S. Solvatochromic and Fluorogenic Dyes as Environment-Sensitive Probes: Design and Biological Applications. *Acc. Chem. Res.* **2017**, *50*, 366−375.
(54) Tai, S.-H.; Lee, W.-T.; Lee, A.-C.; Lin, Y.-W.; Hung, H.-Y.; Huang, S.-Y.; Wu, T.-S.; Lee, E.-J. Therapeutic window for YC-1 following glutamate-induced neuronal damage and transient focal cerebral ischemia. *Mol. Med. Rep.* **2018**, *17*, 6490−6496.

DOI: 10.1021/acscentsci.9b00539
ACS Cent. Sci. 2019, 5, 1541−1553